# Influence of Hydrated Lime on the Self-Healing Capacity of Cement Mortars

*Franco* Grosso Giordano[1*], *Nico* Boon[1], and *Nele* De Belie[2]

[1]Ghent University, Center for Microbial Ecology and Technology (CMET), Coupure Links 653, B-9000 Ghent, Belgium
[2]Ghent University, Magnel-Vandepitte Laboratory, Dept. of Structural Engineering and Building Materials, Technologiepark Zwijnaarde 60, B-9052, Ghent, Belgium

**Abstract.** The capacity of hydrated lime to reabsorb $CO_2$ as it hardens has made it a desirable replacement for cement to produce mortars with an overall lower environmental footprint. Still, research into lime-cement formulations remains limited, especially when it comes to their self-healing capacity.
Some studies show that hydrated lime can improve self-healing in cement mixes, but addition rates are low. Here we present how high lime-cement ratios influence the self-healing capacity of lime mortars. Four mixes of increasing lime-cement ratios were cracked with tensile loading and placed under 1 hour wet, 23 hours dry cycles to stimulate self-healing. The mix design of 50 % lime-50 % cement volume (L50C50) showed self-healing abilities and was tested against a pure cement mixture (L0C100). Microscopy and water flow tests were performed at a cracking age of 7 days and then again after 28 days of healing in three regimes.
Overall, submersion was the best healing regime for both L0C100 and L50C50 and crack self-healing was close to total (100 ± 1 % and 98 ± 6 %, respectively). Nevertheless, the water flow tests show that self-healing in L50C50 was in fact less efficient than that of the L0C100, achieving a 39 ± 21 % reduction in water flow versus 86 ± 11 %.

## 1 Introduction

The study of self-healing in cement-based materials is a field that has developed extensively over the last decades [1–3]. Self-healing is the process whereby microcracks in cementitious materials close or heal on their own accord. Cement is a material that is capable of self-healing autogenously, i.e. that it is an intrinsic capacity of the material. This is argued to be an important mechanisms in extending the service life of the material, reducing long-term costs of maintenance, and, in-turn, making the material more sustainable. As concrete is the most used construction material in the world, the cement industry is turning to more sustainable alternatives to reduce its carbon footprint [4]. The use of recycled aggregates from old construction waste [5], supplementary cementitious material like fly ash and alkali-activated materials [6] are a few steps taken in this direction. Also, new ways of improving the self-healing capacity of cements are being looked into such as the use of additives like SAPs, and techniques such as the use of 3D-printed internal matrices and formulations [7]. The use of hydrated lime has recently come into the spotlight as an interesting substitute that provides a lower carbon footprint to cement. As hydrated lime reabsorbs $CO_2$ over its lifetime, it presents and opportunity of creating construction materials that have an overall lower global footprint. In the realm of self-healing, cement-hydrated lime mixes have been studied to a limited extent and under mostly low addition levels [8–10]. Yildirim [8] looked at how the 2.5% and 5% addition of hydrated lime could be used to supplement the hydration reactions of unhydrated fly ash particles. Meanwhile, Qureshi [9] studied the impact of quicklime ranges of 2.5 % to 10 % on the autogenous self-healing of Portland cements. On the other end of the spectrum, de Nardi [11] explored, amongst others, how a mix of hydrated lime-natural hydraulic lime performed with or without the addition of cement micro-capsules. Hydraulic lime mortars have also seen research but are beyond the scope of this work due to their different chemical reactions. Meanwhile, Gulbe [10] looked at the addition of up to 10 % cement in hydrated lime mortars for historic purposes on its effect on self-healing. Overall, there was a positive association of addition of hydrated lime to cement in terms of self-healing capacity.

Here we studied how the replacement of 25 %, 50 % and 75 % in volume of a cement mortar by lime changed the autogenous self-healing capacity of the mortar. Cracks were created using tensile tests on mortar specimens cast with a central reinforcement bar. The mortar mixtures were then placed under 1 hour wet, 23 hours dry cycles to stimulate self-healing and the multiple cracks were scanned to determine the best healing mortar. The selected mortar was then further tested in comparison with a pure cement mortar. Self-healing was determined using microscopy and water

* Corresponding author: franco.grossogiordano@ugent.be

flow tests (as per [12]) were used to determine the regain in durability of the healed cracks. Cracks were created at 7 days, while three different healing regimes, being water-cycles, submersion and carbonation chamber, were tested.

## 2 Methodology

### 2.1 Mortar formulations and experimental plan

Four mortar formulations were tested of different volume ratios (Table 1) of CEM II A/L 32.5R and a hydrated lime CL 90-S. The bulk densities were 1042 kg/m$^3$ and 426 kg/m$^3$, respectively. The water/binder ratio was determined according to EN 1015-2, to achieve a flow value of 175 ± 10 mm.

Casting was performed as per EN 1015-11 according to the total mass of lime in the binder. For L66C33, a predominately lime mix, due to limitations with the moulds, gauze and filter paper were placed on only one side. Each formulation was cured according to their lime/cement composition as determined by the EN 1015-11.

**Table 1.** Formulation composition and respective water/binder (w/b) ratios.

| Formulation | Lime (ml) | Cement (ml) | w/b in volume |
|---|---|---|---|
| L0C100 | 0 | 280 | 0.7 |
| L33C66 | 93 | 186 | 0.75 |
| L50C50 | 140 | 140 | 0.725 |
| L66C33 | 186 | 93 | 0.725 |

Two experimental series were performed to assess the self-healing capacity of the lime-cement formulations. The first series used a tensile test for crack formation to induce cracks of varying size in all lime-cement mixes. Microscopy was used to assess the progression of self-healing before and after placement in a healing regime.

The second series used water permeability tests, alongside microscopy, to characterize the regain in durability and progression of the self-healing of the best performing lime-cement mix against a pure cement reference.

### 2.2 Tensile tests for crack formation

Tensile tests were used to test the self-healing capacity of the different formulations. For this, one specimen per formulation was cast in moulds of 30x30x360 mm³ with a central reinforcement bar of 6 mm in diameter and ~ 480 mm in length. The samples were cured for 7 days. Then, the ends of the reinforcement bar of the 30x30x360 mm³ prisms were clamped and tensile loaded using an Instron universal testing machine at a loading rate of 0.01 mm/s. The displacement measured during loading was used to have an indication of the final width of the cracks. These varied between ~100-600 µm. Microscopy was used to assess the crack width before and after self-healing.

### 2.3 Water permeability tests

Water permeability tests were used to assess the durability regain on the best self-healing lime-cement formulation. For this, a water flow setup was used and samples were prepared according to Van Mullem [12]. Briefly, three specimens per formulation were cast in 40x40x160 mm³ moulds with a reinforcement bar of 5 mm to create a cast-in-hole. The bar was removed during demoulding and at day 6 after casting the cast-in-hole was enlarged to 6 mm. Tubing was inserted 10 mm into the sampled and glued. The opposite side was sealed. Carbon fiber plates of 39x160 mm$^2$ were then glued on the bottom side of the prisms. At day 7, each prism was cracked using three point bending. The crack was adjusted to an approximate target crack width of 300 µm using a metal clamp. After clamping, aluminium tape was placed over the sides of the crack and a further two carbon fiber plates of 20x140 mm$^2$ were glued on either side of the specimens to retain the crack in place. The epoxy glue was allowed to dry for 24 hours and the crack width was re-measured to calculate the final value. Lastly, samples were submerged in water for 24 hours prior to testing for water permeability using a water flow setup [12]. The main divergences were that water was allowed to flow for 30 s prior to measuring and weight measurements were taken every 30 s for 5 minutes.

### 2.4 Microscopy

Crack widths were measured using an optical microscope (Leica DMC 2900). Three locations on each crack were photographed, and 30 measurements on each zone were taken. The average for the crack was calculated from the average of each zone. Finally, the average crack width of the series was the average of all cracks for that formulation.

### 2.5 Healing regimes

After cracking, tensile test samples were assessed with microscopy, and water permeability test samples for microscopy and water flow tests. Then they were placed in healing regimes for 28 days. Three healing regimes were tested overall. A wet/dry cycle was used for the first round of experiments on tensile test samples, and water submersion and carbonation chamber regimes were added for the subsequent testing series.

Wet/dry cycles consisted of 1 hour submerged and 23 hours under standard curing conditions (65 % relative humidity and 20 °C room temperature). The submersion regime involved leaving samples fully submerged throughout the whole experiment. Tap water was used in both cases. Lastly, the carbonation chamber regime involved leaving samples in a 1 % $CO_2$ atmosphere (20

°C and 65 % relative humidity) throughout the healing period.

# 3 Results

## 3.1 Self-healing behavior of lime-cement formulations under wet/dry cycles

Tensile tests were used to create several cracks in order to have a high throughput study of the self-healing capacity of the formulations under 28 days of wet/dry cycles. Of all the tested samples, healing was observed partially on L50C50 cracks. All other formulations showed no healing (Table 2) including L0C100 which was used as a reference.

**Table 2.** Average crack width, healing percentage and number of cracks for the tested formulations

| Formulation | Average crack width of series (mm) | | Healing percentage | N° of cracks |
|---|---|---|---|---|
| | Day 0 | Day 28 | | |
| L0C100 | 0.28 ± 0.12 | No change | 0 % | 4 |
| L33C66 | 0.59 ± 0.12 | No change | 0 % | 5 |
| L50C50 | 0.12 ± 0.05 | 0.10 ± 0.06 | 16 % | 7 |
| L66C33 | 0.19 ± 0.06 | No change | 0 % | 5 |

Tensile tests also gave some indications of the change in material properties by the replacement of cement with lime. L0C100 mixtures showed drop in force at each instance when cracks were formed in the long prism (Fig. 1). This is due to the high strength and brittleness of cement mortar. Meanwhile, as lime is added to the mortar, these drops in the force-displacement graph shrink (in the case for L33C66) and, when higher percentages of lime are present, disappear entirely from the graph. The addition of lime creates a more ductile material that does not have the same strength as cement. As such, all the tension is placed on the reinforcement bar of the prism rather than on the mortar.

The lower strength also had experimental implications when trying to create cracks that were of similar sizes. On stronger mixes, once cracks were created, the tensile load would increase the size of these cracks. On the other hand, with lower strength mortars, new cracks would readily form as the samples were put under continuous loading, preventing the widening of the cracks and rather creating more cracks (as seen from L50C50, Table 2). This could have had an effect on determining the efficiency of healing of these mortars, as measurements were performed on smaller cracks which heal better. An option to overcome this was to reload the samples after the cracks were created but the results were inconsistent. As such, experimental planning was continued with L50C50 formulations.

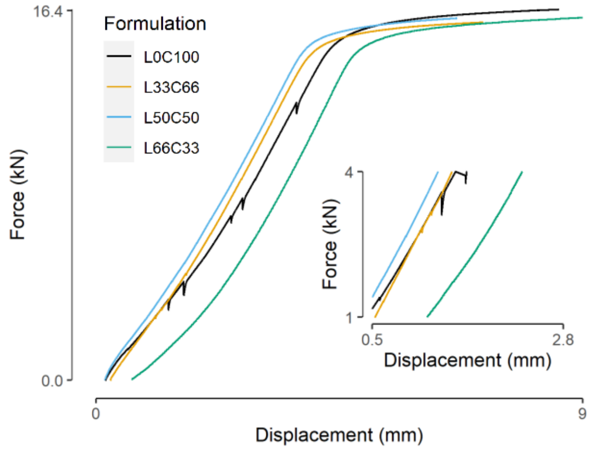


**Fig. 1.** Force-displacement curves for the different formulations. Drops in force indicate formed cracks . Insert shows these drops are also present in L33C66 although of smaller magnitude. More ductile formulations like L50C50 and L66C33 do not have such drops.

## 3.2 Self-healing behavior of L50C50 and L0C100 under different healing regimes

Microscopy and water flow tests were used to measure self-healing on one selected formulations, L50C50, and L0C100 as a reference. Using two different techniques provides an overall better understanding of the self-healing dynamics than a single test.

### *3.2.1 Microscopy tests*

Under this setup, microscopic observation of the samples shows change in crack width and formation of precipitate on both formulations and in all regimes (Fig. 2). Submersion was the most effective healing regime with almost full crack closure observed in all L0C100 (100 ± 1 %) and L50C50 samples (98 ± 6 %). The water cycle and carbonation chamber regime were instead much more limited in stimulating self-healing. L0C100 was outperformed by L50C50 samples in wet-dry cycles (23 ± 3 % vs 33 ± 14 %, respectively), although the self-healing was inconsistent, as seen from the large standard deviation in the mean percent closure. As for the carbonation chamber, both formulations had similar, and limited, self-healing (21 ± 1 % for L0C100, 20 ± 2 % for L50C50).

### *3.2.2 Water flow tests*

Microscopy is an indicative of self-healing at the surface but fails to provide insights into the durability of such healing. Instead, water permeability tests provide a better image of the overall healing of the crack as they provide an understanding of the internal crack filling and durability of the healing products. Specifically, the water flow test has been devised in order to create a more standardized test for the study of self-healing [12].

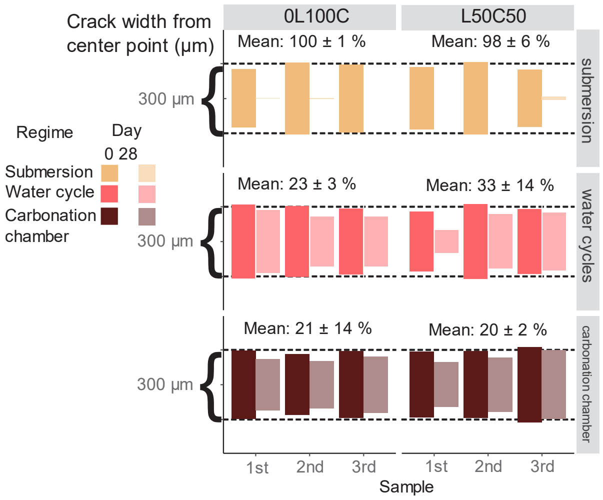


**Fig. 2.** Crack widths before and after 28 days under healing regimes. Average crack healing and standard deviation (in %) are shown above the bars.

Water flow tests on L0C100 samples associate strongly with what was observed under the microscope, where an average 86 ± 11 % healing was observed in the series (Fig. 3). Despite that for L50C50 submersion was the most effective healing regime, the durability regain was much more limited when compared to the results obtained from microscopy. Whereas an almost full crack closure was observed under the microscope, the extent at which these precipitates reduce the flow of water was of 39 ± 21 %.

For wet/dry regimes the observation of a crack width reduction, also failed to correlate to a similar drop in water flow. L0C100 samples did see a significant reduction in water flow in 2 of 3 samples although to a much more limited extent (16 ± 4 %) compared to the virtually total reduction in flow of the submerged samples. L50C50 prisms cured in water cycles showed no significant reduction in water flow even though on average they showed more extensive crack closure than cement samples.

Last but not least, the most consistent results were observed on samples under the carbonation regime where an unexpected increase in water flow was observed on all samples of all formulations. Both L0C100 and L50C50 saw a crack shrinkage, though small, which is counterintuitive to the increased water flow (12 ± 3 % and 22 ± 6 % increase, respectively). It is likely that this is an effect from internal changes in the morphology of the crack which further highlights the importance of multiple techniques to determine self-healing dynamics in mortars. The utilization of techniques that can determine the internal structural soundness of the material, either through visualization like micro-computed tomography or inference through UPV or resonant frequency tests, are important to create a better image of how self-healing works.

## 4 Discussion

The overall better regain in durability of the L0C100 mix over the L50C50 can be attributed to the products

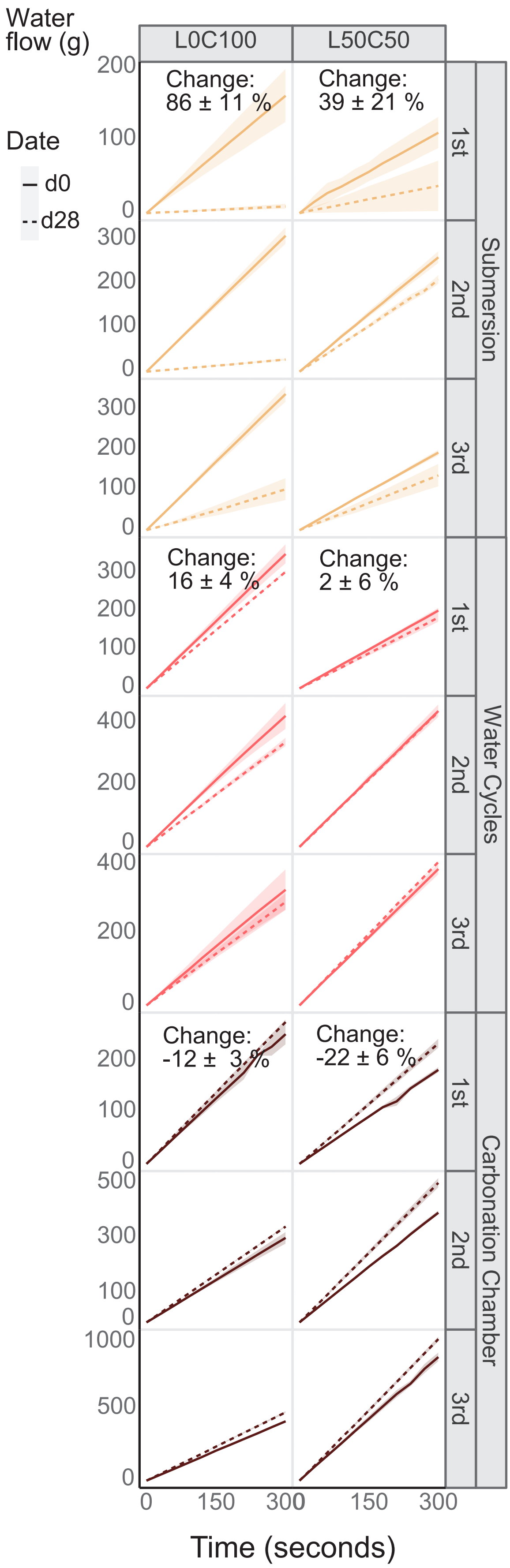


**Fig 3.** Water flow results before and after 28 days under healing regimes. For better visualization the y-axis is not fixed.

of self-healing. Cement is known to react under hydration reactions producing C-S-H and C-A-H while lime carbonates into $CaCO_3$. The former are known for their higher strengths and as such cracks healed with hydration products are expected to be stronger. Although self-healing is usually attributed to the precipitation of $CaCO_3$, the early age at which samples were cracked, that of 7 days, is likely favouring the formation of healing products of C-S-H and C-A-H over $CaCO_3$ in L0C100 samples. As such, these will be stronger than those in the L50C50, which would probably contain more $CaCO_3$ due to the higher lime content. Still, it is necessary to perform further identification of these phases using SEM-EDS imaging. Secondly, it would be of added value to test how these formulations respond to cracking at a later age by curing samples for 28 days. This would help isolate the effect of lime on self-healing, mainly by allowing the hydration reaction to continue while a higher percentage of lime remains unreacted [13]. Also, the process of dissolution and reprecipitation of $CaCO_3$ would be present at a later age. It is important to note, that these reactions do not occur during the permeability tests as the test is performed in a short time span. The test helps isolate the effect on self-healing attributed to the healing regimes. Nevertheless, in a service condition, the process of dissolution and reprecipitation will have a much more active role such as indicated in Seymour [14].

The lack of correlation between the regain in durability and the microscopy observations also highlights the need of techniques that can determine the internal structural soundness of the material, either through visualization like micro-computed tomography or inference through ultrasonic pulse velocity or natural resonant frequency test. It is likely that these differences, at times contradicting such as the case of the samples in the carbonation regime, arise from internal changes in the morphology of the crack which further highlights the importance of multiple techniques to determine self-healing dynamics in mortars. For example, the geometry of the crack have been reported to influence the healing efficiency [15]. This would also support why very few cracks were healed in the initial tensile crack forming tests. Comparing and correlating different tests for self-healing in a systematic manner would prove a valuable step for the field of self-healing mortars.

## 5 Conclusion

In conclusion, we presented the first insights into the self-healing capabilities of cement mortars with high volume replacement by lime. Initial results show that visually, cement and lime-cement mixes heal similarly yet the cement self-healing products show better mechanical properties. As such, the replacement of cement with half the volume of lime does not improve the self-healing capabilities when cracked at an early age. Nonetheless, further testing is required to understand how late age cracks heal, where hydration reactions would be less dominant in the self-healing reactions and dissolution and re-precipitation reactions would play a bigger role.

## References

1. Lee Y.S., W. Park, Appl. Microbiol. Biotechnol. **102** (7), 3059–3070 (2018).
2. De Muynck W., A. Maury, N. De Belie, S. Matthys, (2008).
3. Li W., B. Dong, Z. Yang, J. Xu, Q. Chen, H. Li, F. Xing, Z. Jiang, Adv. Mater. **30** (17), 1705679 (2018).
4. Naqi A., J.G. Jang, Sustain. 2019, Vol. 11, Page 537. **11** (2), 537 (2019).
5. Makul N., R. Fediuk, M. Amran, A.M. Zeyad, G. Murali, N. Vatin, S. Klyuev, T. Ozbakkaloglu, Y. Vasilev, Cryst. 2021, Vol. 11, Page 232. **11** (3), 232 (2021).
6. Provis J.L., Cem. Concr. Res. **114** 40–48 (2018).
7. Sidiq A., R. Gravina, F. Giustozzi, Constr. Build. Mater. **205** 257–273 (2019).
8. Yildirim G., M. Sahmaran, H.U. Ahmed, J. Mater. Civ. Eng. **27** (6), 04014187 (2015).
9. Qureshi T., A. Kanellopoulos, A. Al-Tabbaa, Constr. Build. Mater. **192** 768–784 (2018).
10. Gulbe L., I. Vitina, J. Setina, In: Procedia Engineering. pp. 325–332. Elsevier Ltd (2017).
11. De Nardi C., S. Bullo, L. Ferrara, L. Ronchin, A. Vavasori, Mater. Struct. Constr. **50** (4), 1–12 (2017).
12. Van Mullem T., G. Anglani, M. Dudek, H. Vanoutrive, G. Bumanis, C. Litina, A. Kwiecień, A. Al-Tabbaa, D. Bajare, T. Stryszewska, R. Caspeele, K. Van Tittelboom, T. Jean-Marc, E. Gruyaert, P. Antonaci, N. De Belie, Sci. Technol. Adv. Mater. **21** (1), 661–682 (2020).
13. Cizer O., K. Van Balen, D. Van Gemert, J. Elsen, Proc. Inst. Civ. Eng. Constr. Mater. **162** (1), 19–27 (2009).
14. Seymour L.M., J. Maragh, P. Sabatini, M. Di Tommaso, J.C. Weaver, A. Masic, Sci. Adv. **9** (1), eadd1602- (2023).
15. De Belie N., E. Gruyaert, A. Al-Tabbaa, P. Antonaci, C. Baera, D. Bajare, A. Darquennes, R. Davies, L. Ferrara, T. Jefferson, C. Litina, B. Miljevic, A. Otlewska, J. Ranogajec, M. Roig-Flores, K. Paine, P. Lukowski, P. Serna, J.M. Tulliani, S. Vucetic, J. Wang, H.M. Jonkers, Adv. Mater. Interfaces. **5** (17), 1800074 (2018).